[9] J.-W. Yang, H. R. Harris, M. M. Hussain, B. Sassman, H.-H. Tseng, and R. Jammy, "Enhanced performance and SRAM stability in FinFET with reduced process steps for source/drain doping," in *Proc. IEEE Symp. VLSI Technol., Syst., Appl.*, Apr. 2008, pp. 20–21.
[10] S.-H. Kim and J. G. Fossum, "Design optimization and performance projections of double-gate FinFETs with gate-source/drain underlap for SRAM application," *IEEE Trans. Electron Devices*, vol. 54, no. 8, pp. 1934–1942, Aug. 2007.
[11] S. A. Tawfik and V. Kursun, "Mutual exploration of FinFET technology and circuit design options for implementing compact brute-force latches," in *Proc. IEEE Asia Symp. Quality Electron. Des.*, Jul. 2009, pp. 1–8.

Channel Estimator and Aliasing Canceller for Equalizing and Decoding Non-Cyclic Prefixed Single-Carrier Block Transmission via MIMO-OFDM Modem

Shau-Yu Cheng, Chueh-An Tsai, and Terng-Yin Hsu

***Abstract*—Without a cyclic prefix (CP), most single-carrier (SC) transmissions can not adopt frequency-domain equalizer (FDE) directly. This work utilizes frequency-domain channel estimator (FD-CE) and decision-feedback aliasing canceller (DF-AC) to produce single-FFT SC-FDE. In this way, non-CP single-carrier block transmission (SCBT) can be decoded using sphere decoder of MIMO-OFDM modems to support multimode and backward compatibility under an acceptable complexity in IEEE 802.11 very high throughput (VHT). An N-point FFT is sufficient to measure channel frequency responses (CFR) from L-sample preambles ($L \leqq N/2$). And then, M-bit block codes ($M \leqq L$) are decodable over frequency domains with DF-AC's help. Simulations and measurements imply that this work can ensure adequate performance, even if there is no CP existed against the distortions of multipath propagation.**

***Index Terms*—Aliasing canceller, channel estimator, compatibility, multimode, single-carrier block transmission (SCBT), single-carrier frequency-domain equalization (SC-FDE).**

I. Introduction

In most of the wireless broadband applications like WiMax, Wifi, UWB and WRAN, compensation for multipath fading is highly pointed in order to make systems work properly. With the help of a cyclic prefix (CP), single-input single-output orthogonal frequency-division multiplexing (SISO-OFDM) and multiple-input multiple-output orthogonal frequency-division multiplexing (MIMO-OFDM) systems can be easily integrated. In addition, this can help estimate channels and equalize packets over frequency domains directly. Although single-carrier block transmission (SCBT) without any CP gains throughput, it causes fast Fourier transformation (FFT) aliasing in frequency-domain equalizer (FDE)—FDE can not assure sufficient performance directly. Thus, one of the major challenge for multimode integrations is to make equalizers as compact as possible, i.e., consolidation of non-CP SCBT, SISO OFDM and MIMO OFDM. Reconfigurable and scalable architectures [1], [2] with heterogeneous units are good solutions to support such operations. However, multiple equalizers are built in designs. A single-carrier frequency-domain equalizer (SC-FDE), being an attractive solution, is developed to eliminate FFT aliasing without a circular property in some approaches [3], [4], e.g., overlap-and-save and overlap-and-add methods. Yet, additional DFT units were included. The user defined formats [5]–[7], inserting CP into single-carrier datum against the multipath propagation, were created to improve performance. SC-FDEs with a pair of FFT and IFFT for IEEE 802.16 [8] and IEEE 802.15.3a with an impulse option [9] were developed to demodulate SCBT with CP over time domains. In the case of single-carrier transmissions with pseudo noise (PN) spreading, a block-based SC-FDE with both DFT and IDFT for HIPERLAN-2 [10] was utilized to yield an additional 3-dB gain, and it was also demodulated in the time domain.

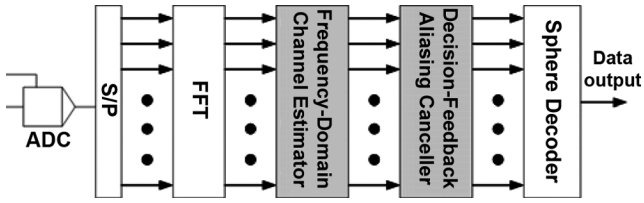

Fig. 1. Block diagram of the proposed single-FFT SC-FDE for sharing with an MIMO-OFDM modem.

The objective of this study is to derive single-FFT processes for supporting multimode and backward compatibility under an acceptable complexity in MIMO-OFDM modems, such as IEEE 802.11 very high throughput (VHT), with a non-CP SCBT. Fig. 1 displays the block diagram of this work, where the sphere decoder (SD) [11]–[13] is widely adopted in MIMO-OFDM modems. All equalizations and decoding are performed over the frequency domain. An N-point FFT is sufficient to process L-sample preambles and M-bit block codes ($M \leq L \leq N/2$).

The remainder of this paper is organized as follows. The system assumptions with problem statements are addressed in Section II. The proposed single-FFT processes are described in Section III. Performance evaluations are presented in Section IV. Implementations and complexity are discussed in Section V. Finally, Section VI presents our conclusions.

II. System Assumptions

A. System Descriptions

Indoor frequency-selective fading, e.g., IEEE [14] and JTC [15], is assumed to roughly span two symbols of L-sample preambles and M-bit block codes. The proposed packet format of non-CP SCBT is that datum without FEC are encoded by block code (K code sets contain M bits), modulated by QPSK and synchronized via L-sample preambles ($L \geq M$). The j^{th} received signal can be expressed as

$$\mathbf{r}_j = \mathbf{H}_L \mathbf{s}_j + \mathbf{H}_U \mathbf{s}_{j-1} + \mathbf{n}_0 \tag{1}$$

where $\mathbf{r}_j$ is the j^{th} $2L \times 1$ received vector, $\mathbf{n}_0$ is $2L \times 1$ complex additive white Gaussian noise (AWGN) vector with variance σ_n^2, and $\mathbf{S}_j$ is the j^{th} $L \times 1$ transmitted symbol, e.g., preambles, single-carrier (SC) block codes, or multicarrier datum with $N - L$ zeros. $\mathbf{H}_{2L \times 2L}$ is the circulant Toeplitz matrix with the first column being $\mathbf{h}$ and $\mathbf{h} = [h_0, h_1, \ldots, h_{2L-1}]$ denotes a channel impulse response (CIR). Both

Manuscript received July 23, 2008; revised December 29, 2008. First published October 06, 2009; current version published December 27, 2010.This work was supported in part by the National Science Council of Taiwan, under Grant NSC 98-2220-E-009-004. This work was conducted under "A plan to actively participate in international standard organizations for wireless communications" of the Institute for Information Industry, MOEA.

The authors are with the Department of Computer Science, National Chiao Tung University, Hsinchu 300, Taiwan (e-mail: tyhsu@cs.nctu.edu.tw; shauyu.cheng@msa.hinet.net; catsai@csie.nctu.edu.tw).

Digital Object Identifier 10.1109/TVLSI.2009.2031137

$\mathbf{H}_L$ and $\mathbf{H}_U$ are the lower triangle (including diagonal entries) matrix and upper triangle matrix of $\mathbf{H}_{2L\times 2L}$, respectively

$$\mathbf{H}_{2L\times 2L}=\begin{bmatrix} h_0 & h_{2L-1} & \cdots & \cdots & h_1 \\ h_1 & h_0 & \ddots & \ddots & \vdots \\ \vdots & h_1 & \ddots & h_{2L-1} & h_{2L-2} \\ \vdots & \vdots & \ddots & h_0 & h_{2L-1} \\ h_{2L-1} & h_{2L-2} & \cdots & h_1 & h_0 \end{bmatrix}. \quad (2)$$

B. Problem Statements

Linear convolution of two finite sequences is commonly conducted by multiplying the fast Fourier transforms of these two zero-padding input sequences. In SISO-OFDM and MIMO-OFDM systems, the channel frequency response (CFR) can be obtained from the FFT of the received symbol with CP divided by the FFT of the transmitted sequences [16]

$$\begin{aligned} R_k &= H_k\cdot C_k + n_k \Rightarrow \hat{H}_k \\ &\approx \frac{R_k}{C_k},\ k\in\{0,1,\ldots,N-1\} \end{aligned} \quad (3)$$

where N is the FFT size, C_k is the k^{th} element of the frequency response of transmitted sequence, H_k is the k^{th} element of real CFR, and $\hat{H}_k$ is the k^{th} element of estimated CFR. In frequency-selective fading, the CFR is not an identity matrix. One problem associated with single-FFT processes for non-CP SCBT is to extend the FFT size in order to be enough to cover the entire packet. For a finite FFT size, it is impossible to gain a linear convolution of non-CP symbols and channel directly. Another consideration is that most zero-forcing equalizers are adversely affected by noise enhancement due to CFR with zeros or very small values (deep fading) [13], [15].

III. Single-FFT Processes

A. Frequency-Domain Channel Estimator

Based on the received vector in (1), the linear convolution of the j^{th} symbol and the CIR can be deconstructed into two parts: one is *body*, denoted by $\mathbf{H}_L\mathbf{s}_j$, and the other is $\mathbf{H}_U\mathbf{s}_j$, caused by *interblock interference* (IBI). In receivers, the body part of the current symbol convolved with the CIR is mixed with the IBI term of previous symbols in each FFT window. These two components can be separated for linear convolution over the time domain, namely *preamble reconstruction*. Taking all possibilities of QPSK modulations, the preambles (training symbols) are multiplied by complex coefficient. If "1" is the basis, the other three cases, i, -1 and $-i$ can be written as $c_2\cdot 1$, $c_3\cdot 1$, and $c_4\cdot 1$, where c_2 is i, c_3 is -1 and c_4 is $-i$. Two useful combinations of convolved vectors are

$$\begin{cases} \mathbf{y}' = c_1\cdot\mathbf{H}_L\mathbf{b} + c_2\cdot\mathbf{H}_U\mathbf{b} \\ \mathbf{y}'' = c_3\cdot\mathbf{H}_L\mathbf{b} + c_4\cdot\mathbf{H}_U\mathbf{b}, \quad c_1\neq c_3 \text{ or } c_2\neq c_4 \end{cases} \quad (4)$$

where $\mathbf{b}$ is the $L\times 1$ base vector of modulated preambles. Via (1), the received signals can be rewritten as

$$\begin{cases} \mathbf{r}' = \mathbf{y}' + \mathbf{n}' = c_1\cdot\mathbf{H}_L\mathbf{b} + c_2\cdot\mathbf{H}_U\mathbf{b} + \mathbf{n}' \\ \mathbf{r}'' = \mathbf{y}'' + \mathbf{n}'' = c_3\cdot\mathbf{H}_L\mathbf{b} + c_4\cdot\mathbf{H}_U\mathbf{b} + \mathbf{n}'' \end{cases} \quad (5)$$

and the body part and the IBI term can be found by

$$\begin{cases} \mathbf{H}_L\mathbf{b} = \frac{c_4\cdot\mathbf{r}'-c_2\cdot\mathbf{r}''}{c_1c_4-c_2c_3} + \frac{-c_4\cdot\mathbf{n}'+\mathbf{c_2}\cdot\mathbf{n}''}{c_1c_4-c_2c_3} \\ \mathbf{H}_U\mathbf{b} = \frac{c_1\cdot\mathbf{r}''-c_3\cdot\mathbf{r}'}{c_1c_4-c_2c_3} + \frac{-c_4\cdot\mathbf{n}'+c_2\cdot\mathbf{n}''}{c_1c_4-c_2c_3}. \end{cases} \quad (6)$$

In (6), each second term is also AWGN. To reduce AWGN effects, $\mathbf{H}_L\mathbf{b}$ and $\mathbf{H}_U\mathbf{b}$ can be obtained as

$$\begin{cases} \mathbf{H}_L\mathbf{b} = \frac{c_4\cdot E[\mathbf{r}']-c_2\cdot E[\mathbf{r}'']}{c_1c_4-c_2c_3} = \frac{c_4\cdot\mathbf{y}'-c_2\cdot\mathbf{y}''}{c_1c_4-c_2c_3} \\ \mathbf{H}_U\mathbf{b} = \frac{c_1\cdot E[\mathbf{r}'']-c_3\cdot E[\mathbf{r}']}{c_1c_4-c_2c_3} = \frac{c_1\cdot\mathbf{y}''-c_3\cdot\mathbf{y}'}{c_1c_4-c_2c_3} \end{cases} \quad (7)$$

where $E[\mathbf{r}']$ and $E[\mathbf{r}'']$ can be individually calculated through averaging the two sets of the received preambles that collect two specific combinations of current and previous symbols defined in (5). After averaging $\mathbf{r}'$ and $\mathbf{r}''$ and solving $\mathbf{H}_L\mathbf{b}$ and $\mathbf{H}_U\mathbf{b}$, the CFR can be measured via one-tap division. The frequency response is

$$\hat{\mathbf{H}}_N[k] = \frac{\mathbf{Y}_N[k]}{\mathbf{B}_N[k]} \quad (8)$$

where $\mathbf{Y}_N = F_N([(\mathbf{H}_L\mathbf{b})^T \quad (\mathbf{H}_U\mathbf{b})^T]^T)_{ze}$, $\mathbf{B}_N = F_N(b)_{ze}$, $\mathbf{F}_N$ is an $N\times N$ Fast Fourier matrix with entries given by $\mathbf{F}_{p,q} = e^{2\pi pqi/N}$, $(\bullet)_{ze}$ represents zero padding for the length of N and $N\geq 2L$. Furthermore, $c_4\cdot\mathbf{y}' - c_2\cdot\mathbf{y}''$ and $c_1\cdot\mathbf{y}'' - c_3\cdot\mathbf{y}'$ are the functions of preamble reconstruction.

B. Decision-Feedback Aliasing Canceller

Based on decision feedback, the j^{th} received datum (in frequency domains) can be rewritten as

$$\begin{aligned} \mathbf{R}_j' &= \mathbf{R}_j - \mathbf{F}_N(\mathbf{H}_U\hat{\mathbf{s}}_{j-1})_{ze} \\ &= \mathbf{F}_N(\mathbf{H}_L\mathbf{s}_j)_{ze} + \mathbf{F}_N(\mathbf{n}_0)_{ze} \end{aligned} \quad (9)$$

where $\mathbf{R}_j \triangleq \mathbf{F}_N(\mathbf{r}_j)_{ze}$ and $\hat{\mathbf{s}}_{j-1}$ is the previous decoded symbol. Similar to MIMO detections, if a maximum-likelihood (ML) decision [17] is applied to decode datum over the frequency domain, the maximum *a priori* (MAP) equals

$$\hat{\mathbf{s}}_j = \arg\min_{\mathbf{d}_j\in\mathbb{C}} \left|\mathbf{R}_j' - \mathbf{F}_N(\mathbf{H}_L\mathbf{d}_j)_{ze}\right|^2 \quad (10)$$

where $\mathbb{C}$ indicates the code set and $\mathbf{d}_j$ is an M-bit block code. Reducing the complexity of implementations and sharing with a MIMO-OFDM modem, an ML decision is replaced by SD. Although CFR $\hat{\mathbf{H}}_N$ is estimated using linear convolution with a preamble reconstruction, the body part and the aliasing term of each ideal code set must be separated for decoding references. Instead of re-transforming to time domains for $\mathbf{H}_L\mathbf{d}_j$ and $\mathbf{H}_U\hat{\mathbf{s}}_{j-1}$, a separation operator $\tilde{\mathbf{G}}$ is constructed to extract $\mathbf{F}_N(\mathbf{H}_L\mathbf{d}_j)_{ze}$ via the linear convolution of $\mathbf{d}_j$ and $\mathbf{h}$

$$\begin{aligned} \mathbf{F}_N(\mathbf{H}_L\mathbf{d}_j)_{ze} &= \tilde{G}F_N(\mathbf{h}\otimes\mathbf{d}_j)_{ze} \\ &= \tilde{\mathbf{G}}\mathbf{D}_H\mathbf{F}_N(\mathbf{d}_j)_{ze} \end{aligned} \quad (11)$$

$$\mathbf{F}_N(\mathbf{H}_U\hat{\mathbf{s}}_j)_{ze} = \mathbf{D}_H\mathbf{F}_N(\hat{\mathbf{s}}_j)_{ze} - \mathbf{F}_N(\mathbf{H}_L\hat{\mathbf{s}}_j)_{ze} \quad (12)$$

where $\otimes$ is the linear convolution and $\mathbf{D}_H = diag\left(\hat{\mathbf{H}}_N[0],\hat{\mathbf{H}}_N[1],\ldots,\hat{\mathbf{H}}_N[N-1]\right)$ is a diagonal matrix containing the CFR. After the channel estimation, multiply $\mathbf{F}_N(\mathbf{d}_j)_{ze}$ by $\mathbf{D}_H$, and pass through the separation operator $\tilde{\mathbf{G}}$—A new coefficient $\mathbf{F}_N(\mathbf{H}_L\mathbf{d}_j)_{ze}$ is produced for sphere decoding. In the time domain, the body part is easily derived by taking the first L of linear convolution

$$\begin{aligned} \mathbf{H}_L\mathbf{d}_j &= \mathbf{G}\cdot(\mathbf{h}\otimes\mathbf{d}_j) \\ \mathbf{G} &= \begin{bmatrix} \mathbf{I}_{L\times L} & \mathbf{0}_{L\times(N-L)} \\ \mathbf{0}_{(N-L)\times L} & \mathbf{0}_{(N-L)\times(N-L)} \end{bmatrix}. \end{aligned} \quad (13)$$

Then separation operator $\tilde{\mathbf{G}}$ can be obtained by (11) and (13)

$$\tilde{\mathbf{G}} = \mathbf{F}_N\mathbf{G}\mathbf{F}_N^{-1}. \quad (14)$$

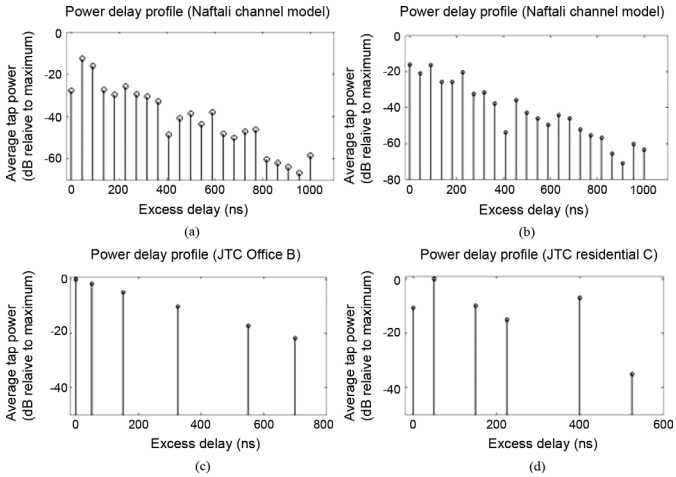

Fig. 2. Power delay profiles for JTC and IEEE channel models. (a) and (b): Two random cases of IEEE model (RMS delay spread is 100 ns). (c): JTC indoor office B model. (d): JTC indoor residential C model.

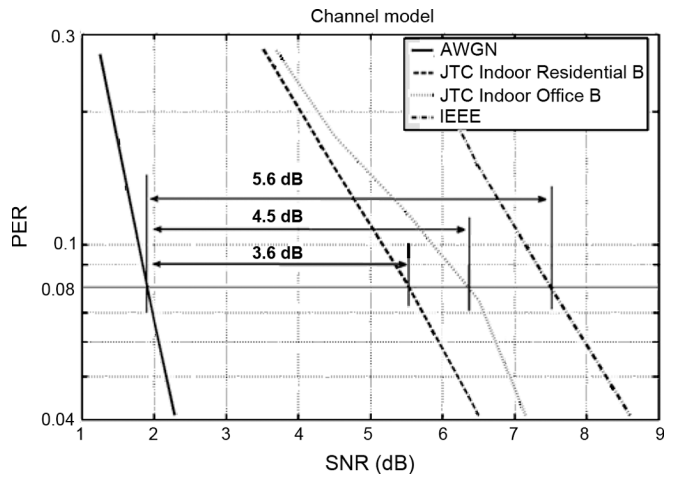

Fig. 3. Simulation of the linear (8, 4) code in IEEE and JTC fading.

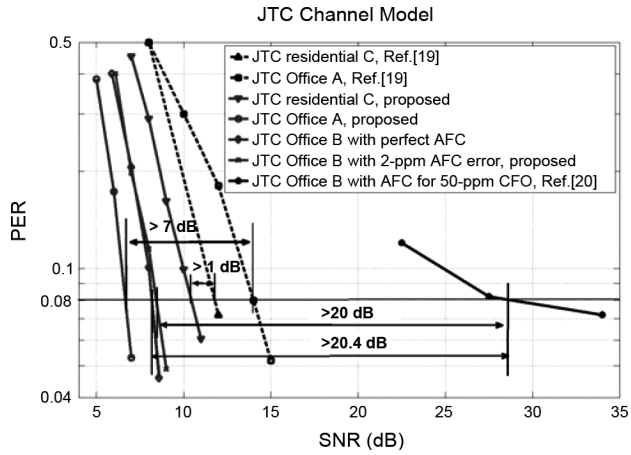

Fig. 4. Simulation of CCK in JTC fading—office A, residential C and office B with residual CFOs.

Each entry value of $\tilde{\mathbf{G}}$ is constant because the matrices of $\mathbf{F}_N$, $\mathbf{G}$ and $\mathbf{F}_N^{-1}$ are fixed. After cancellation of the aliasing term $\mathbf{F}_N(\mathbf{H}_U\hat{\mathbf{s}}_{j-1})_{se}$ of the previous decoded symbol $\hat{\mathbf{s}}_{j-1}$, $\mathbf{s}_j$ is decodable over frequency domains. In the case of decoding the 1^{st} data symbol, $\mathbf{F}_N(\mathbf{H}_U\hat{\mathbf{s}}_{j-1})_{se}$ is acquired prior from the packet header.

IV. Performance Evaluations

The WiFi systems and a linear block codes are used to evaluate the proposed SC-FDE (without FEC), where the FFT size is 64 and the number of preambles is 56. Each preamble, modulated by BPSK, is spreading with 11-chip Barker code ($L = 11$) [14]—two useful combinations of preambles are $\{c_1 = 1,\ c_2 = 1\}$ and $\{c_3 = 1,\ c_4 = -1\}$. Only one antenna is utilized to receive the non-CP SCBT in the MIMO-OFDM modem. The basis of our performance is the packet error rate (PER) that is required to be 8% in frequency-selective fading. Fig. 2 displays the power delay profiles of JTC [15] and IEEE 802.11 [14] (Naftali model: Rayleigh fading with phase distributed uniformly) channel models, which are used to measure the system performance in multipath environment. The packet length is 1024 bytes, encoded by linear (8, 4) code [18] with BPSK modulation and complementary code keying (CCK) [14] with QPSK modulation, respectively. The generator matrix of a linear (8, 4) code is given by

$$\mathbf{H}_{(8,4)} = \begin{bmatrix} 1 & 0 & 1 & 0 & 1 & 0 & 1 & 0 \\ 1 & 1 & 0 & 0 & 1 & 1 & 0 & 0 \\ 1 & 0 & 0 & 1 & 1 & 0 & 0 & 1 \\ 1 & 1 & 1 & 1 & 0 & 0 & 0 & 0 \end{bmatrix}. \tag{15}$$

The minimum hamming distance is 4. In WiFi systems, each CCK codeword (8-bit orthogonal block code) is composed of four phases $\varphi_1, \varphi_2, \varphi_3$ and φ_4 of $\{0, \pi/2, \pi, 3\pi/2\}$ $(M = 8)$.

Fig. 3 plots the PER of the linear (8, 4) code in both JTC and IEEE 802.11 fading channels. Compared with the case of AWGN, our SNR losses are around 3.6 dB $\sim$ 5.6 dB, depending on fading environments. In Fig. 4, the proposed scheme has improved performances compared with some time-domain extents [19], [20]. The simulation results of channel model of JTC indoor office A indicates that the proposed scheme performs better than previous study [19], because the nonlinear equalization employs the sphere decoding with the search of minimum Euclidean distance over transmitted symbols. In the case of JTC indoor residential B, a CFO of 50 ppm with 1-ppm and 2-ppm residual errors caused by automatic frequency control (AFC) is induced in systems. In contrast with the ICI equalizer [20], this proposal also yields an improvement of 20-dB, indicating that the impact of residual CFOs does not make significant performance degradation. By transferring RF signals to MATLAB via USB for real-time measurements before VLSI implementations, XilinxDSP Development Kits with on-board 14-bit A/Ds, 14-bit D/As and FPGA (2-million gates and 50 MHz) are connected to an in-house 2.4 GHz 2×2 RF module with 20-MHz bandwidth to transmit and record real wireless packets. In this way, a software-defined radio (SDR) platform is shown in Fig. 5. The received EVM of QPSK is about -21 dB.

V. Implementations and Complexity

Figs. 6 and 7 show the block diagrams of the proposed FD-CE and single-FFT SC-FDE with DF-AC, respectively. Five key modules are derived in the FD-CE: (1) a preamble reconstruction with pattern recognition for pre-processing linear convolution before FFT; (2) a look-up table (LUT) for storing the ideal frequency responses of preamble; (3) complex multipliers with conjugate output for calculating the linear convolution; and, (4) two averages for reducing AWGN effects. The single-FFT SC-FDE with DF-AC (Fig. 7) contains five major building blocks: (1) an DF-AC to eliminate the FFT aliasing of non-CP symbols; (2) a sphere decoder to decode datum over the frequency domain without noise enhanced; (3) an LUT to save ideal frequency responses

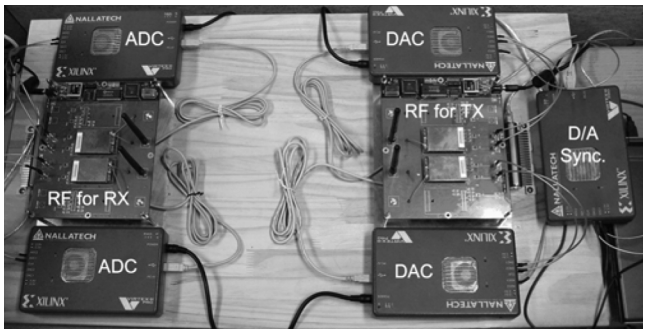

Fig. 5. SDR platform for SCBT measurements.

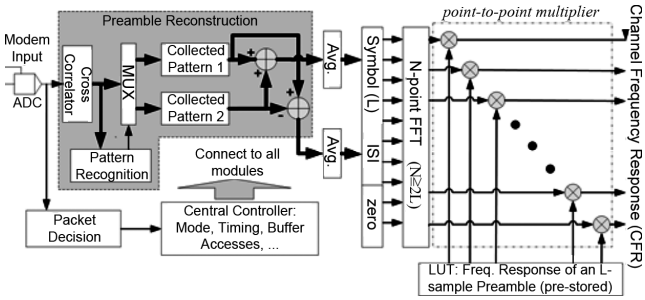

Fig. 6. Block diagram of the proposed FD-CE.

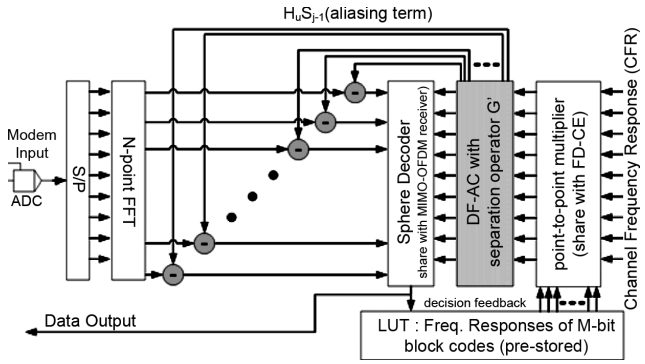

Fig. 7. Block diagram of the single-FFT SC-FDE with DF-AC.

of M-bit block codes as decoding references; and, (4) complex multipliers (shared with FD-CE) to generate new references for sphere decoding.

Fig. 8 displays the detail architecture of a 4×4 MIMO-OFDM modem with the proposed SC-FDE supporting two kinds of packet formats in WiFi systems: (1) DSSS-CCK and (2) MIMO-OFDM. The MIMO-OFDM modem was implemented via hardware-description language (HDL) and mapped on FPGA of a XilinxDSP Development Kit. In Fig. 8, one of the four FFTs based on variable-length FFT architecture [21] supports 32 and 64 points, transferring the reconstructed data to the frequency domain. The preamble reconstruction extracts both body and ISI terms of Barker code to reconstruct linear convolution before FFT. By multiplying the frequency response of reconstructed data with the reciprocal of the frequency response of an ideal preamble (Barker code; pre-stored in ROM1), the channel frequency response (CFR) is extracted. Once the CFR is obtained, the ALU uses the four complex multiplier banks to calculate $\mathbf{D}_H\mathbf{F}_N(\mathbf{d}_j)_{ze}$ and $\mathbf{F}_N(\mathbf{H}_L\mathbf{d}_j)_{ze} = \tilde{\mathbf{G}}\mathbf{D}_H\mathbf{F}_N(\mathbf{d}_j)_{ze}$ for all $\mathbf{d}_j$, where $\mathbf{d}_j$ is the frequency response of an ideal CCK code and $\tilde{\mathbf{G}}$ is the matrix operator (both saved in the ROM2). For all CCK codes, each output of $\mathbf{D}_H\mathbf{F}_N(\mathbf{d}_j)_{ze}$ and the body $(\mathbf{F}_N(\mathbf{H}_L\mathbf{d}_j)_{ze})$ and aliasing terms $(\mathbf{F}_N(\mathbf{H}_U\mathbf{d}_j)_{ze})$ are stored in SRAM1 and SRAM2, respectively. If the received signals are data symbols, CE flag is set to 0. Then, the received signals subtract from an aliasing term with the feedback code index in SRAM2 to get the body term of the received signals. Finally, the sphere decoder with four SD engines [22] decodes the body term of received signals and feeds back the decision for next decoding.

The bottlenecks of the data path are the computations of $\mathbf{F}_N(\mathbf{H}_L\mathbf{d}_j)_{ze} = \tilde{\mathbf{G}}\mathbf{D}_H\mathbf{F}_N(\mathbf{d}_j)_{ze}$ and $\mathbf{D}_H\mathbf{F}_N(\mathbf{d}_j)_{ze}$ for all $\mathbf{d}_j$, where $\mathbf{d}_j$ is the ideal frequency response of the j^{th} CCK code and $\tilde{\mathbf{G}}$ is the matrix operator (both saved in the ROM2). Because only the code set with zero phase ones needs to be calculated and $\tilde{\mathbf{G}}$ is the circular matrix with the first column $[\tilde{g}_0, \tilde{g}_{N-1}, \ldots, \tilde{g}_2, \tilde{g}_1]$, ($\tilde{g} = 0$ if i is even; $\tilde{g}_i = a_i + b_i i$ and $\tilde{g}_{N-i} = a_i - b_i i$ for $1 \le i \le 15$), the computing complexity of $\mathbf{D}_H\mathbf{F}_N(\mathbf{d}_j)_{ze}$ and $\mathbf{F}_N(\mathbf{H}_L\mathbf{d}_j)_{ze}$ of 256 CCK codes can be reduced to 32^*64 and 9^*32^*64 complex multiplications, respectively. To balance with processing time, clock rate and complexity, there are 32 complex multipliers to build 4 multiplier banks, shared with MIMO OFDM and SCBT. At the top right of Fig. 8, it shows the computing order of 32 complex multipliers for $\mathbf{F}_N(\mathbf{H}_L\mathbf{d}_j)_{ze}$ in DSSS-CCK modes. $\mathbf{D}_H\mathbf{F}_N(\mathbf{d}_j)_{ze}$ and each body/aliasing term are then stored in SRAM1 and SRAM2, respectively. The processing time of $\mathbf{D}_H\mathbf{F}_N(\mathbf{d}_j)_{ze}$ and $\mathbf{F}_N(\mathbf{H}_L\mathbf{d}_j)_{ze}$ is 12.8 us or 13 Barker codes at 50-MHz clock rate. Due to packet detection and synchronizations, the number of available preambles for preamble reconstruction is about 27.

Furthermore, the classical SD for MIMO detection includes two stages: 1) the preprocessing of QR decomposition and 2) a tree search of depth-first branch and bound (B&B) algorithm. In order to support both MIMO-OFDM and SCBT modes, three parts of SD have been modified, which are the preprocessing, metric computation and tree structure. Instead of the preprocessing of QR decomposition in MIMO-OFDM mode, the preprocessing of SCBT decoding is to calculate the body term $(\mathbf{F}_N(\mathbf{H}_L\mathbf{d}_j)_{ze})$ and aliasing term $(\mathbf{F}_N(\mathbf{H}_U\mathbf{d}_j)_{ze})$ by using the shared multiplier banks. The metric computation of SCBT decoding which is simpler than that of MIMO detection requires subtraction between two complex signals' vectors. Furthermore, unlike each parent node to extend Q possible child nodes in the tree structure of Q-QAM MIMO detection, the parent node can only extend one child node except the root node in the tree structure of SCBT decoding. If the partial Euclidean distance of current node is larger than the upper bound, a dead end is declared and the next start node of backward recursion is always one of the child nodes of root. Because the behavior of tree punching also follows the depth-first B&B algorithm in SCBT mode, the SD search engine does not require additional modifications. The main overhead of such SD is the control unit to handle all data paths in VLSI implementations. The clock rate and the number of SD engines are dominated by 64-QAM MIMO detection of a 4×4 MIMO-OFDM modem that four SD engines with 150-MHz clock rate are utilized in this design. The decoding latency of CCK using a 150-MHz SD engine is less than 720 ns, so it met DSSS-CCK decoding requirements (CCK symbol duration is 720 ns). By partitioning CCK into four sub-sets decoded via four parallel SD engines, we can reduce the decoding latency to 40 cycles or we can slow down the clock rate to 100 MHz.

The hardware complexity is summarized in Table I. The 0.3% for combination logics, 33.3% for SRAM and 99% ROM are only used in DSSS-CCK mode, which indicates the additional cost making a 4×4 MIMO-OFDM modem support non-CP SCBT is memory (SRAMs and ROMs). Although the total ROM size for the DSSS-CCK mode is 7760 bytes, the major cost of ROMs is just the address decoder. Most combinational logics are shared with MIMO-OFDM and DSSS-CCK modes,

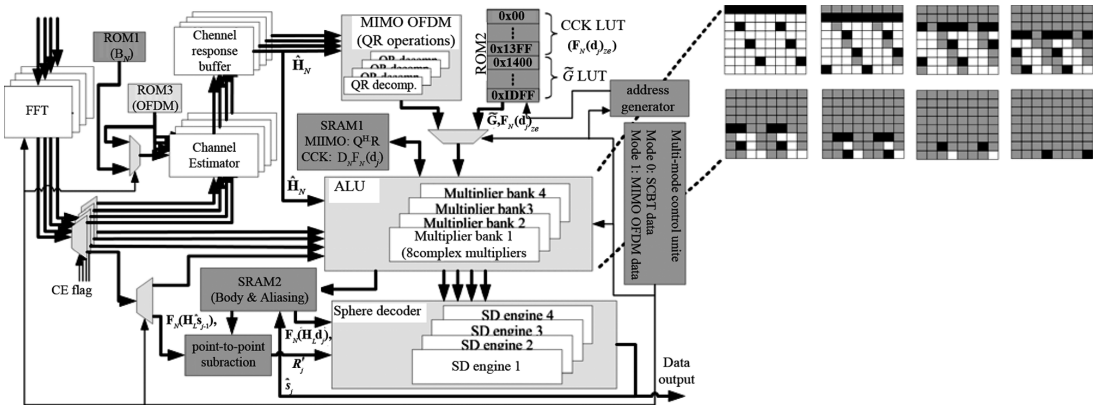

Fig. 8. Detail architecture and complexity of a 4 × 4 MIMO-OFDM modem with the proposed SC-FDE (top right for the rule of signal multiplications of $\tilde{\mathbf{G}}$; dark squares for the elements being currently computed, and light squares for the elements after calculated).

TABLE I
VLSI COMPLEXITY OF A 4 × 4 MIMO-OFDM MODEM

Modules	# of Gates (K)	Ratio	Modes
Channel estimator	22	1.5%	Shared
Complex multipliers	3.5*32=112	7.7%	Shared
Sphere decoder	260x4=1,040	71.3%	Shared
QR operations	70*4=280	19.2%	MIMO-OFDM
Preamble reconst.	5	0.3%	SC-FDE
SRAM	**Size (bytes)**	**Ratio**	**Modes**
SRAM 1	10,240	66.7%	Shared
SRAM 2	5,120	33.3%	SC-FDE
ROM	**Size (bytes)**	**Ratio**	**Modes**
ROM1	80	1%	SC-FDE
ROM2	7,680	98.%	SC-FDE
ROM3	80	1%	MIMO-OFDM

e.g., channel estimators, FFTs, complex multipliers and SD engines. Hence, the additional complexity compared with conventional multimode systems is acceptable.

VI. CONCLUSION

The contributions of this work are to design and implement the proposed FD-CE and DF-AC for providing the equalization and decoding of non-CP SCBT over frequency domains. Only one N-point FFT $(M \leq L \leq N/2)$ is required to make the SC-FDE integrate with an MIMO-OFDM modem efficiently, ensuring IEEE 802.11VHT multimode and backward compatibility. Evaluations of a linear (8, 4) code and WiFi in frequency-selective fading indicate that all results satisfy 8% PER to assure adequate performance within acceptable complexity. Moreover, this work is also corresponded to Giga-bit wireless specification discussed in IEEE 802.15.3c to support OFDM and non-OFDM packet accesses.

REFERENCES

[1] A. Chun, E. Tsui, I. Chen, H. Honary, and J. Lin, "Application of the Intel@ reconfigurable communication architecture to 802.11a, 3G and 4G standards," in *Proc. IEEE Symp. Emerging Technol.*, May 2004, pp. 659–662.

[2] J. Hoffman, D. A. Ilitzky, A. Chun, and A. Chapyzhenka, "Architecture of the scalable communications core," in *Proc. IEEE Symp. Networks-on-Chip*, 2007, pp. 40–52.

[3] P. A. Dmochowski and P. J. McLane, "Frequency domain equalization for high data rate multipath channels," in *Proc. IEEE Pacific Rim Conf.*, Aug. 2001, vol. 2, pp. 534–537.

[4] J. J. Shynk, "Frequency-domain and multirate adaptive filtering," *IEEE Signal Process. Mag.*, vol. 9, no. 1, pp. 14–37, Jan. 1992.

[5] J. H. Jang, H. C. Won, and G. H. Im, "Cyclic prefixed single carrier transmission with SFBC over mobile wireless channels," *IEEE Signal Process. Lett.*, vol. 13, no. 5, pp. 261–264, May 2006.

[6] M. Morelli, L. Sanguinetti, and U. Mengali, "Channel estimation for adaptive frequency-domain equalization," *IEEE Trans Wireless Commun.*, vol. 4, no. 5, pp. 2508–2518, Sep. 2005.

[7] Y. Zhu and K. B. Letaief, "Single carrier frequency domain equalization with time domain noise prediction for wideband wireless communications," *IEEE Trans Wireless Commun.*, vol. 5, no. 12, pp. 3548–3557, Dec. 2006.

[8] D. Falconer, "Frequency domain equalization for single-carrier broadband wireless systems," *IEEE Commun. Mag.*, pp. 58–66, Apr. 2002.

[9] Y. Wang, X. Dong, P. H. Wittke, and S. Mo, "Cyclic prefixed single carrier transmission in ultra-wideband communications," *IEEE Trans. Wireless Commun.*, vol. 5, no. 8, pp. 2017–2021, Aug. 2006.

[10] N. Benvenuto and S. Tomasin, "On the comparison between OFDM and single carrier modulation with a DFE using a frequency-domain feedforward filter," *IEEE Trans. Commun.*, vol. 50, no. 6, pp. 947–955, Jun. 2002.

[11] K. Wong, C. Tsui, R.-K. Cheng, and W. Mow, "A VLSI architecture of a K-best lattice decoding algorithm for MIMO channels," in *Proc. IEEE ISCAS*, 2002, vol. 3, pp. 273–276.

[12] M. O. Damen, H. E. Gamal, and G. Caire, "On maximum-likelihood detection and the search for the closest lattice point," *IEEE Trans. Inf. Theory*, vol. 49, no. 10, pp. 2389–2402, Oct. 2003.

[13] T. D. Chiueh and P. Y. Tsai, *OFDM Baseband Receiver Design for Wireless Communications*. New York: Wiley, 2007.

[14] B. O'Hara and A. Petrick, *IEEE 802.11 Handbook: A Designer's Companion*, 2 ed. Piscataway, NJ: IEEE Press, 2005.

[15] K. Pahlavan and A. H. Levesque, *Wireless Information Networks*. New York: Wiley, 1995.

[16] J. Terry and J. Heiskala, *OFDM Wireless LANs: A Theoretical and Practical Guide*. Indianapolis, IN: Sams, 2002.

[17] G. Ungerboeck, "Adaptive maximum-likelihood receiver for carrier-modulated data-transmission systems," *IEEE Trans Commun.*, vol. 22, no. 5, pp. 624–636, May 1974.

[18] S. Lin and D. J. Costello, *Error Control Coding: Fundamentals and Applications*. Englewood Cliffs, NJ: Prentice Hall, 1983.

[19] S. W. Gerstacker, C. Jonietz, and R. Schober, "Equalization for WLAN IEEE 802.11b," in *Proc. IEEE Int. Conf. Commun.*, Jun. 2004, vol. 6, pp. 20–24.

[20] K. Barman and A. V. Malipatil, "ICI equalizer in a CCK based DSSS communication system," *Proc. TENCN*, vol. 4, pp. 15–17, Oct. 2003.

[21] R. Pandey and M. L. Bushnell, "Architecture for variable-length combined FFT, DCT and MWT transform hardware for multimode wireless system," in *Proc. IEEE Int. Conf. Embedded Syst.*, Jan. 2007, pp. 121–126.

[22] A. Burg, M. Borgmann, M. Wenk, M. Zellweger, W. Fichtner, and H. Bolcskei, "VLSI implementation of MIMO detection using the sphere decoding algorithm," *IEEE J., Solid-State Circuits*, vol. 40, no. 7, pp. 1566–1577, Jul. 2005.